PNAS RESEARCH ARTICLE | PLANT BIOLOGY

The Na^+/H^+ antiporter SALT OVERLY SENSITIVE 1 regulates salt compensation of circadian rhythms by stabilizing GIGANTEA in *Arabidopsis*

Joon-Yung Cha[a,b,1], Jeongsik Kim[c,d,1], Song Yi Jeong[a], Gyeong-Im Shin[a], Myung Geun Ji[a,b], Ji-Won Hwang[a], Laila Khaleda[a], Xueji Liao[a], Gyeongik Ahn[b], Hee-Jin Park[e], Dong Young Kim[f], Jose M. Pardo[g], Sang Yeol Lee[a], Dae-Jin Yun[h,i], David E. Somers[d], and Woe-Yeon Kim[a,b,2]

Edited by Xinnian Dong, Duke University, Durham, NC; received May 6, 2022; accepted July 14, 2022

The circadian clock is a timekeeping, homeostatic system that temporally coordinates all major cellular processes. The function of the circadian clock is compensated in the face of variable environmental conditions ranging from normal to stress-inducing conditions. Salinity is a critical environmental factor affecting plant growth, and plants have evolved the SALT OVERLY SENSITIVE (SOS) pathway to acquire halotolerance. However, the regulatory systems for clock compensation under salinity are unclear. Here, we show that the plasma membrane Na^+/H^+ antiporter SOS1 specifically functions as a salt-specific circadian clock regulator via GIGANTEA (GI) in *Arabidopsis thaliana*. SOS1 directly interacts with GI in a salt-dependent manner and stabilizes this protein to sustain a proper clock period under salinity conditions. SOS1 function in circadian clock regulation requires the salt-mediated secondary messengers cytosolic free calcium and reactive oxygen species, pointing to a distinct regulatory role for SOS1 in addition to its function as a transporter to maintain Na^+ homeostasis. Our results demonstrate that SOS1 maintains homeostasis of the salt response under high or daily fluctuating salt levels. These findings highlight the genetic capacity of the circadian clock to maintain timekeeping activity over a broad range of salinity levels.

circadian clock | GI | protein stabilization | salt compensation | SOS1

Significance

The circadian clock is an endogenous molecular timekeeper that coordinates biological rhythms of physiological and developmental processes in living organisms. Compensation of the circadian clock plays a crucial role in maintaining constant periodicity in fluctuating diurnal environments. Although ion contents in plants fluctuate daily or seasonally due to changes in transpiration rates and soil moisture, the precise molecular mechanisms of salt compensation are not well established. We report that SOS1 is essential for maintaining the circadian clock period under saline conditions and mediates salt compensation by directly protecting GI. These results suggest that plants may have recruited the GI protein to coordinate homeostatic functions against various levels of salt stress via the salt-dependent association between GI and individual SOS proteins.

Circadian clocks regulate many developmental and physiological processes. In plants, the phase and period of the circadian clock are adjusted by environmental information such as light, temperature, and nutrient input (1). The circadian clock in *Arabidopsis thaliana* is an interlocking transcriptional feedback loop composed (in part) of CIRCADIAN CLOCK ASSOCIATED1/LATE ELONGATED HYPOCOTYL (CCA1/LHY) and TIMING OF CAB2 EXPRESSION1 (TOC1), two key elements of the core oscillator (2). The posttranslational regulatory mechanisms of the circadian clock include control of the protein stability of plant-specific evening components such as GIGANTEA (GI) and ZEITLUPE (ZTL). GI acts as a cochaperone with HEAT SHOCK PROTEIN90 (HSP90) to stabilize ZTL and sustains the rhythmic oscillation of this F-box protein to promote the targeted degradation of TOC1 and PSEUDO RESPONSE REGULATOR5 (PRR5) (3–5).

An essential property of the circadian system is period compensation of the central circadian clock against abiotic stresses, including thermal stress, allowing it to maintain a robust, accurate rhythm in the face of environmental fluctuations within physiological ranges (6, 7). Multiple key clock molecules are involved in temperature compensation at different temperature ranges through transcriptional, posttranscriptional, and posttranslational regulation (8), suggesting that period compensation might be established by recruiting different clock components under various stress conditions. GI and ZTL are also crucial factors for thermal adaptation of the clock to increasing temperature ranges by counterbalancing *CCA1* and *LHY* expression and protein quality control mechanisms with HSP90, respectively (9, 10). A thermo-dependent GI–ZTL interaction is also involved in the dynamic changes in ZTL levels for temperature compensation (11).

Various circadian clock components are involved in plant responses to diverse stresses. The *prr5,7,9* mutant is tolerant to freezing, salt, and drought stress (12); *gi* is tolerant to salt and oxidative stress (13, 14); transgenic plants with RNA interference–induced silencing of *TOC1* are tolerant to drought stress (15); and plants overexpressing *CCA1* are tolerant to oxidative stress (16). GI is involved in the SALT OVERLY SENSITIVE (SOS) pathway, which is essential for salt-stress tolerance in *Arabidopsis* (17). The Ca^{2+}-binding protein SOS3 perceives salt-mediated cytosolic calcium ($[Ca^{2+}]_{cyt}$) signals and recruits the serine/threonine protein kinase SOS2 to the

The authors declare no competing interest.

This article is a PNAS Direct Submission.

See online for related content such as Commentaries.

[1]J.-Y.C. and J.K. contributed equally to this work.

[2]To whom correspondence may be addressed. Email: kim1312@gnu.ac.kr.

This article contains supporting information online at http://www.pnas.org/lookup/suppl/doi:10.1073/pnas.2207275119/-/DCSupplemental.

Published August 8, 2022.

plasma membrane (18). The SOS2–SOS3 complex activates the Na^+/H^+ antiporter SOS1 by phosphorylation, which triggers the export of sodium ions and thus confers salt-stress tolerance (17–19). Under normal growth conditions, GI represses SOS2-based activation of SOS1 by sequestering SOS2 via a direct interaction. Salt stress induces the proteasomal degradation of GI, resulting in the activation of SOS1 via the release of SOS2 (13), which explains the salt-induced inhibition of flowering (20).

Although reciprocal regulation between the circadian clock and abiotic stress responses has been reported, the molecular mechanisms underlying their interconnection remain unclear. Here, we present molecular and genetic evidence for salinity compensation in the circadian clock, which enables plants to maintain robust rhythms and accurate timing over a broad range of physiological salinity levels. We demonstrate that SOS1 plays an unique regulatory role in the circadian clock by compensating the effects of salt on the circadian period through the stabilization of GI protein.

Results

SOS1 Functions in Salt Compensation. Since GI is involved in both maintaining the circadian clock and acquiring salt tolerance, we reasoned that the SOS system might function in the response of the circadian clock to salinity via an effect on GI. To investigate this notion, we assessed the circadian rhythm of a *CAB2* promoter-luciferase reporter (*CAB2-LUC*) in individual *Arabidopsis sos1-sos3* mutants (21). The period was lengthened in *sos1-1* plants in the presence of 25 mM NaCl, whereas the periods in *sos2-2* and *sos3-1* were not significantly different from that of the wild-type (WT; Col-*gl*) (Fig. 1 *A* and *B*). In the absence of salt, the *CAB2-LUC* periods of all *sos* mutants were similar to those of the WT (Fig. 1 *C* and *D*). In addition, the period of *CAB2-LUC* in the *sos1-1* background increased with increasing concentrations of NaCl up to 25 mM NaCl under both blue and red light conditions (Fig. 1 *E* and *F* and *SI Appendix*, Fig. S1). Because the *sos1-1* mutant is hypersensitive to NaCl (19), we did not treat plants with NaCl levels higher than 50 mM.

We validated these results using *sos* mutant plants harboring *CCA1-LUC* or mesophyll protoplasts of individual mutants transiently expressing *CCA1-LUC* (*SI Appendix*, Fig. S2). Under 25-mM NaCl, only *sos1-1* showed a significantly longer period than WT (*SI Appendix*, Fig. S2 *A* and *B*), which is consistent with the *CAB2-LUC* results (Fig. 1 *A* and *B*). *sos1-1* protoplasts subjected to high salt (154 mM NaCl) also showed longer periods relative to WT or other *sos* mutants (*SI Appendix*, Fig. S2 *C* and *D*). These results indicate that SOS1

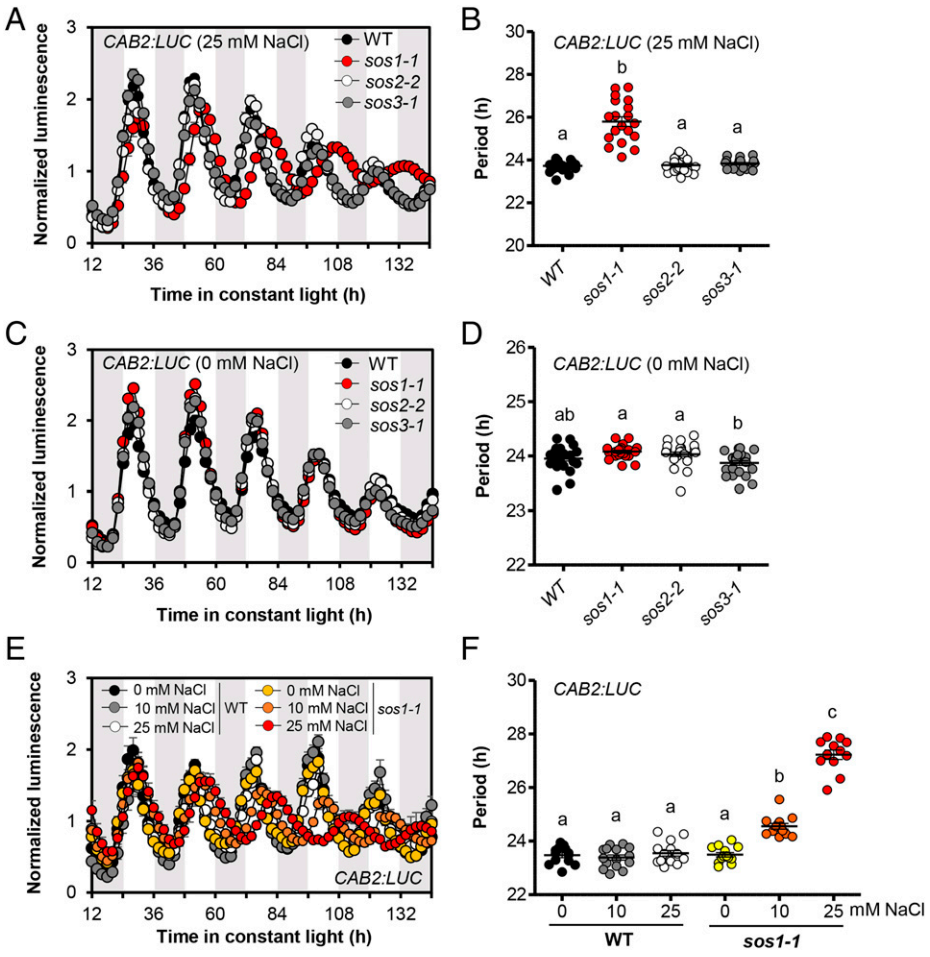

Fig. 1. SOS1 is essential for maintaining circadian clock in response to increasing salinity. (*A–D*) *CAB2-LUC* activity monitored in WT (Col-gl, $n = 22$ for *A* and *B*; $n = 26$ for *C* and *D*), *sos1-1* ($n = 19$; $n = 24$), *sos2-2* ($n = 19$; $n = 26$), and *sos3-1* ($n = 20$; $n = 24$) seedlings in the presence (*A* and *B*) or absence (*C* and *D*) of 25 mM NaCl under constant blue light (31 μmol m^{-2} s^{-1}). (*E* and *F*) NaCl concentration–dependent *CAB2-LUC* activity examined in WT seedlings treated with 0 mM ($n = 13$), 10 mM ($n = 15$), or 25 mM NaCl ($n = 15$) and *sos1-1* seedlings treated with 0 mM ($n = 13$), 10 mM ($n = 13$), or 25 mM NaCl ($n = 12$). (*A*, *C*, and *E*) Bioluminescence traces (normalized to the mean expression level over 12- to 144-h sampling schedule) and (*B*, *D*, and *F*) period estimates (means ± SEM) of LUC reporter activity. Different characters indicate that the means are significantly different between genotypes or treatments ($P < 0.05$, one-way ANOVA with Tukey's multiple comparisons test). *n* refers to the number of monitored plants.

is essential for proper clock function under physiological salt concentrations. Since salt-dependent period lengthening in *sos1* was consistent under both blue and red light conditions (Fig. 1 *E* and *F* and *SI Appendix*, Fig. S1), blue or white light conditions were used for experiments thereafter.

Regulatory Role of SOS1 in Protecting GI. The lengthened period in *sos1-1* under saline conditions might be due to the aberrant expression of central clock components (22, 23). Thus, we examined the transcriptional expression of core circadian clock genes in WT and *sos1-1* plants by qRT-PCR. These core oscillator genes, including *CCA1* and *TOC1*, were not affected by salt treatment in WT or *sos1-1* plants (*SI Appendix*, Fig. S3), suggesting that the altered period in *sos1-1* is not due to the transcriptional regulation of core circadian clock genes.

Since GI is degraded upon salt exposure in a proteasome-dependent manner and some *gi* mutations alter the circadian period (13, 24), we examined whether the long period in *sos1-1* under saline conditions is due to the degradation of GI by *sos1* mutation–mediated salt signaling. At physiological salt levels (50 mM NaCl), GI levels decreased in *sos1-1* but not in WT, *sos2-2*, or *sos3-1* (Fig. 2 *A* and *B*), consistent with their circadian rhythm phenotypes. In addition, GI abundance in *sos1-1* was hypersensitive to NaCl levels compared to the WT (*SI Appendix*, Fig. S4).

GI stabilizes ZTL, an F-box–type E3 ubiquitin ligase that recruits TOC1 for proteasomal degradation (3, 25). Hence, we examined ZTL and TOC1 protein levels in WT and *sos1-1*. As expected, ZTL levels dramatically decreased and TOC1 levels increased in *sos1-1* under salt treatment, whereas no salt-dependent changes in ZTL or TOC1 protein levels were observed in the WT (Fig. 2 *C*–*F*). These data suggest that the *sos1* mutation reduces GI levels under saline conditions, leading to low ZTL levels and a long circadian period (25). Since both salt-dependent period lengthening and destabilization of GI only occurred in *sos1-1* mutant, not in WT, clock periods and GI protein abundance were monitored in *sos1* mutant backgrounds thereafter.

Salt-Dependent Interaction between SOS1 and GI. We previously demonstrated that in the absence of salt, GI predominantly interacts with SOS2 and associates with SOS2 and SOS3, but not with SOS1 (13). Thus, we hypothesized that GI associates with SOS1 in a salt-dependent manner. We tested this notion by examining *Nicotiana benthamiana* leaves transiently coexpressing GI and SOS1 in the presence or absence of 100 mM NaCl over a 12-h time series. SOS1–green fluorescent protein (GFP) coimmunoprecipitated with GI- hemagglutinin (HA) at higher affinity at 3 to 9 h after infiltration in 100 mM NaCl (Fig. 3*A*). Bimolecular fluorescence complementation (BiFC) assays confirmed the interaction between GI and SOS1 under 100 mM NaCl treatment in vivo (Fig. 3*B*). We demonstrated that GI directly interacts with the cytoplasmic tail of SOS1 (SOS1C, residues 453 to 1,146) in a glutathione *S*-transferase

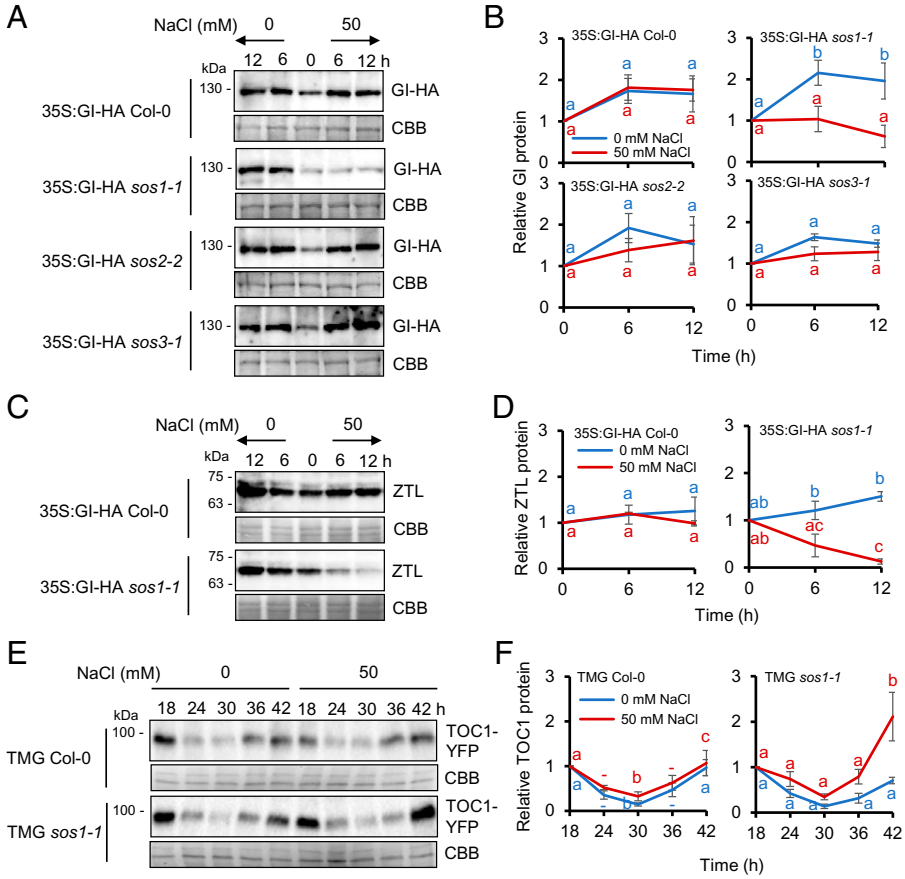

Fig. 2. SOS1 enhances GI protein accumulation in response to saline conditions. (*A*–*F*) Protein abundance of GI (*A* and *B*), ZTL (*C* and *D*), and TOC1 (*E* and *F*) in response to saline conditions. Ten-day-old seedlings grown in 12-h white light/12-h dark cycle were treated with water (as a control) or 50 mM NaCl at ZT0 and harvested at the indicated time points after treatment. GI-HA, ZTL, and TOC1-YFP were detected with α-HA, α-ZTL, and α-GFP antibodies, respectively. Blots are representative of GI-HA (*A*), ZTL (*C*), or TOC1-YFP (*E*) shown from three (GI-HA, *B*; ZTL, *D*) or four (TOC1-YFP, *F*) biological replicates quantified relative to a Coomassie brilliant blue (CBB)-stained gel portion. Data represent means ± SEM, and different characters indicate significantly different between treatments or time periods ($P < 0.05$, one-way ANOVA with Tukey's multiple comparisons test; –, not significant compared with the data at ZT18).

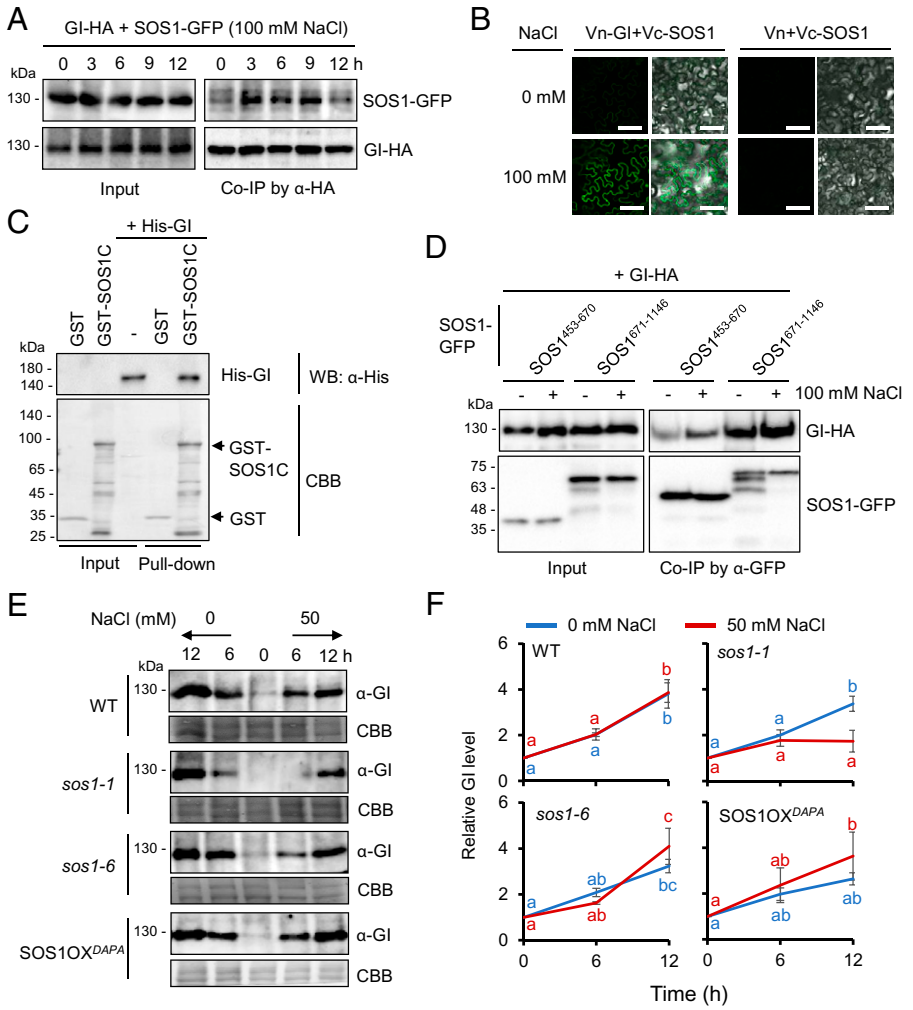

Fig. 3. GI association with SOS1 is salt-dependent. (*A* and *B*) GI–SOS1 interaction under salt-stress (100 mM NaCl) conditions examined by Co-IP analysis using coexpression of GI-HA and SOS1-GFP (*A*) and BiFC analysis using coexpression of the N-terminal fragment of Venus (Vn)-GI and the C-terminal fragment of Venus (Vc)-SOS1 or Vn and Vc-SOS1 (*B*) in *N. benthamiana* epidermal cells. Control (0 mM NaCl) was examined by infiltration of water in BiFC analysis. Scale bars, 100 μm. (*C*) GST pull-down assay. Bacterially expressed GST and GST-SOS1C (amino acids 453 to 1,146) were independently immobilized onto Glutathione Sepharose 4 beads and incubated with purified His-GI. Coeluted His-GI was verified with α-His antibody. WB, Western blot analysis; CBB, Coomassie brilliant blue staining. (*D*) Interaction between GI and C-terminal truncated variants of SOS1 ($SOS1^{453-670}$ and $SOS1^{671-1146}$). Co-IP analysis was carried out using transient coexpression of truncated variants of SOS1 with GFP tag and GI-HA in *N. benthamiana* epidermal cells with or without 100 mM NaCl. (*E* and *F*) Protein abundance of GI in different *sos1* alleles under saline conditions. Ten-day-old seedlings grown in 12-h white light/12-h dark cycle were treated with water (as a control) or 50 mM NaCl at ZT0 and harvested at the indicated time points after treatment. Endogenous GI protein (*E*) was detected with α-GI antibody. All blots are representative of each set of trials; quantification of GI levels (*F*) relative to CBB-stained gel portion is shown in the graphs with means ± SEM, $n = 3$. Different characters indicate that the means are significantly different between treatments or time periods ($P < 0.05$, one-way ANOVA with Tukey's multiple comparisons test).

(GST) pull-down assay (Fig. 3*C*). Therefore, SOS1 associates with GI in a salt-dependent manner.

SOS1 is a 1,146–aa protein with 12 transmembrane domains at the N-terminal region and a long cytosolic tail containing a domain with high sequence similarity to AtNHX8 (residues 441 to 739 in SOS1), followed by SOS1/NHX7–specific sequences comprising a putative cyclic nucleotide-binding domain (residues 740 to 1,146) and an auto-inhibitory domain (residues 1,005 to 1,044) (19, 26, 27) (*SI Appendix*, Fig. S5). We constructed two truncated variants of the SOS1 cytosolic tail spanning residues 453 to 670 ($SOS1^{453-670}$) and 671 to 1,146 ($SOS1^{671-1146}$) tagged with GFP at the C terminus and coexpressed them with GI-HA in *N. benthamiana* (Fig. 3*D* and *SI Appendix*, Fig. S5). GI coimmunoprecipitated with $SOS1^{671-1146}$ independently of NaCl treatment (Fig. 3*D*). By contrast, the GI–$SOS1^{453-670}$ interaction was stronger in the presence versus the absence of 100 mM NaCl.

We assessed the effectiveness of the interaction between GI and a portion of the C terminus of SOS1 by measuring GI protein abundance in other salt-sensitive *sos1* alleles (19). These included *sos1-1*, with a frameshift created by a 14-bp deletion (1,330 to 1,343) resulting in a premature stop codon at amino acid 298 of SOS1, and *sos1-6*, with a G3652A nucleotide change resulting in a premature stop at amino acid 578 (*SI Appendix*, Fig. S5). The *sos1-6* mutant, which produces the truncated SOS1 protein containing the 453 to 577 SOS1–GI association region, showed normal GI accumulation under both normal and saline conditions, like WT (Fig. 3 *E* and *F*). These results indicate that the 453- to 577-aa region of SOS1, comprising half of the AtNHX8-like domain of SOS1, is essential for salt-dependent interaction with and stabilization of GI. GI accumulation in $SOS1OX^{DAPA}$ plants, in which the Na^+/H^+ exchanger activity of SOS1 was inactivated by phosphosite mutations at S1136 and S1138, was not affected by salt treatment, although the salt sensitivity of $SOS1OX^{DAPA}$ plants was comparable to that of *sos1-1* (27) (Fig. 3 *E* and *F*). Therefore, neither the phosphorylation of SOS1 by SOS2 kinase nor salt tolerance is required for GI stabilization. Instead, these data suggest that

the physical interaction with the AtNHX8 domain of the SOS1 C-terminal region is required for GI stabilization under saline conditions.

Regulatory Role of SOS1-Mediated Ca^{2+} and Reactive Oxygen Species (ROS). Salt stress is accompanied by additional intracellular stresses such as osmotic stress and ion toxicity, primarily due to low water availability and nutrient imbalance in the cytosol, respectively (28). Thus, we investigated whether the effect of salt on the circadian clock and GI stabilization in *sos1* is mediated by salt itself or by salt-induced secondary stresses. The lengthened circadian period of *CAB2-LUC* and destabilized GI protein in the *sos1-1* background in response to salt was not recapitulated by treatment with mannitol (an osmotic stress inducer) or KCl (an ion toxicity inducer) (*SI Appendix*, Fig. S6). We then examined the possible roles of secondary signaling molecules such as Ca^{2+} and ROS in the SOS1-mediated circadian period and GI abundance regulation, as plant cells generate intracellular Ca^{2+} and ROS signals by salt stress (29, 30). In the absence of *SOS1*, 10 mM $CaCl_2$ treatment (like 50 mM NaCl treatment) prevented GI accumulation, whereas the addition of ethylene glycol tetraacetic acid (EGTA) strongly inhibited this effect (*SI Appendix*, Fig. S7). These results indicate that salt-induced increases in $[Ca^{2+}]_{cyt}$ negatively regulate GI accumulation under saline conditions.

$[Ca^{2+}]_{cyt}$ increases in response to Ca^{2+} release from internal reservoirs via cyclic adenosine diphosphate ribose (cADPR) signals and/or influx from extracellular fluid (31, 32). Thus, we treated plants with nicotinamide [an antagonist of cADPR signaling (33)] or $GdCl_3$ [an inhibitor of extracellular Ca^{2+} influx (34)] to inhibit the increase in $[Ca^{2+}]_{cyt}$ under saline conditions. The longer period of *CAB2-LUC* and GI destabilization in *sos1-1* under saline conditions were completely rescued by adding 1 mM and 50 mM nicotinamide, respectively (Fig. 4 *A*–*C*). Exogenous 50 μM $GdCl_3$ treatment partially rescued the effects of salt on lengthening the circadian period and destabilizing GI protein in *sos1-1* (Fig. 4 *D*–*F*). In addition, blocking salt-induced ROS accumulation by treatment with the synthetic antioxidant dimethylthiourea (DMTU) rescued the lengthened circadian period and GI degradation in *sos1-1* (*SI Appendix*, Fig. S8). Nicotinamide, $GdCl_3$, or DMTU alone did not alter circadian oscillations (32) (*SI Appendix*, Fig. S9). In addition, GI-SOS1 interaction is enhanced by $CaCl_2$ or methyl viologen (a ROS generator) as well as NaCl (*SI Appendix*, Fig. S10). These data suggest that salt-responsive $[Ca^{2+}]_{cyt}$ and ROS regulate the circadian clock's proper functioning and GI protein abundance in the absence of SOS1.

***gi-1* Is Epistatic to *sos1-1* in Response to Salinity Conditions.** The lengthened circadian period in *sos1* mutants was accompanied by low GI levels under all conditions examined. The dysfunction of GI alters the amplitude and period of the circadian clock in several *gi* mutants of *Arabidopsis*; *gi-1* (an allele having truncated GI proteins of 1,002 amino acids instead of native GI proteins with 1,173) displays a short period, while *gi-2* (a null allele with truncated GI protein of 144 amino acids) does a long period (24, 35). To investigate whether the altered GI protein levels in *sos1* are responsible for the change in the period under saline conditions, we explored the genetic relationship between *SOS1* and *GI* in circadian clock regulation using WT, *gi-1*, *sos1-1*, and *sos1-1gi-1* plants, because the long period of the *gi-2* allele is similar to that of *sos1-1*. In the absence of salt, the rhythm of *CAB2-LUC* in *sos1-1gi-1* was not significantly different from that in WT (Fig. 5 *A* and *C*). In the presence of salt, however, the long period of *sos1-1* was rescued to the shorter periods of WT, *gi-1, or sos1-1 gi-1* (Fig. 5 *B* and *C*). These results indicate that *gi-1* is epistatic to *sos1-1*, suggesting that SOS1 is essential for maintaining the circadian clock via GI stabilization in response to changing salinity conditions. We note that the short period of *gi-1* may be due to an altered function of a truncated GI protein. We further tested the stronger, long period *gi-2* allele and found NaCl did not lengthened period (*SI Appendix*, Fig. S11), consistent with the expected effect of salinity lengthening period through reduced GI levels in an *sos1-1* null background. Collectively, these findings indicate that the role of SOS1 in protecting GI helps maintain proper clock functioning in the face of daily fluctuations in salinity levels.

Discussion

Here, we identified an unexpected function of SOS1 as a regulator of salt compensation to maintain circadian clock period. We propose that the molecular mechanism behind this function hinges on SOS1 protecting GI from salt-mediated degradation. *Arabidopsis* is not particularly salt tolerant (36), but its circadian period is relatively stable over the physiological range of salt levels. Mutation of *SOS1* leads to a longer circadian period in response to increased salt levels but has no effect on this period in the absence of salt application (37) (Fig. 1 and *SI Appendix*, Fig. S1). The SOS1–GI interaction is salt dependent (Fig. 3 *A* and *B*), and the degradation of GI in response to low salt levels (e.g., 25 mM) occurs in *sos1* mutants but not in WT or *sos2-2* or *sos3-1* mutants (Fig. 2 *A* and *B* and *SI Appendix*, Fig. S4). In accordance with the GI levels in *sos1*, ZTL abundance is lower and TOC1 abundance is higher in the mutant compared to the WT (Fig. 2 *C*–*F*), resulting in a longer free-running period. In addition, genetic analysis indicated that *gi* is epistatic to *sos1* with respect to circadian period (Fig. 5 *A* and *B*), indicating that the effect of SOS1 is GI dependent. These findings suggest that the direct protection of GI protein by SOS1 against mild salt stress contributes to salt compensation in plants.

SOS1 functions as a Na^+/H^+ antiporter to export Na^+ ions from the cytosol and might also act as a regulator or sensor under salt stress (38). This is akin to the nitrate transporter NRT1.1 and the hexokinase HXK1, which have dual functions as enzymes and key sensors for their substrates (39–41). We provide several lines of evidence for a regulatory or sensory role of SOS1. First, the protection of GI by SOS1 against salt is independent of the action of SOS2 and SOS3, which work together to activate SOS1. Accordingly, GI degradation under salt was detected in some salt-sensitive *sos1* alleles (e.g., *sos1-1* and *sos1-10*) but not in others (e.g., *sos1-6* or $SOS1OX^{DAPA}$ in Fig. 3 *E* and *F*), which differed in the retention or absence of the AtNHX8-like C-terminal domain of SOS1/NHX7. Second, the interaction between GI and SOS1 is salt dependent and is mediated by the AtNHX8-like domain of SOS1 (Fig. 3*D*). Third, the effect of SOS1 in period compensation was observed at low physiological levels of salt (e.g., 10 mM NaCl), below the stressful salt level (Fig. 1 *E* and *F* and *SI Appendix*, Fig. S1). In high-salt conditions, SOS1 fails to protect GI against salt, which releases SOS2 from the GI–SOS2 complex and activates the antiporter function of SOS1 to reduce the salt level in the cell. Therefore, we propose a dual homeostatic role for SOS1 as a regulator of salt compensation under normal conditions and as a Na^+/H^+ antiporter for exporting excess salt under salt stress (Fig. 6) (13).

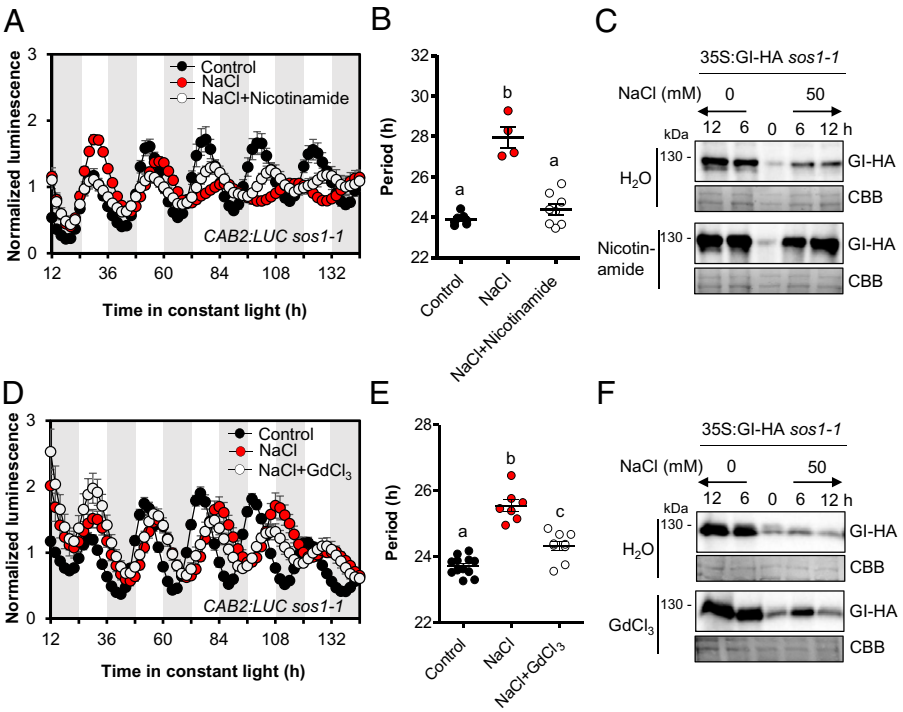

Fig. 4. Salt-induced calcium release regulates the circadian clock and GI protein abundance in *sos1*. (*A*, *B*, *D*, and *E*) Rhythms of LUC reporter activity of *CAB2:LUC* monitored in *sos1-1* seedlings treated with water (Control, $n = 7$ for *A* and *B*; $n = 12$ for *D* and *E*), 25 mM NaCl ($n = 4$ for *A* and *B*; $n = 7$ for *D* and *E*), 25 mM NaCl plus 1 mM nicotinamide ($n = 8$; *A* and *B*), or 25 mM NaCl plus 50 μM $GdCl_3$ ($n = 9$; *D* and *E*) under constant blue light (31 μmol m^{-2} s^{-1}). (*A* and *D*) Bioluminescence traces. Each bioluminescence dataset was normalized to the mean expression level over 12- to 144-h sampling schedule. (*B* and *E*) Period estimates (means ± SEM) for LUC reporter activity. Different characters indicate that the means are significantly different between treatments ($P < 0.05$, one-way ANOVA with Tukey's multiple comparisons test). *n* refers to the number of monitored plants. (*C* and *F*) Blocking of salt-induced GI degradation in *sos1-1* by treatment with calcium release inhibitors. Ten-day-old *35S:GI-HA sos1-1* seedlings were incubated with water (as a control) or 50 mM NaCl in the absence or presence of 50 mM nicotinamide (*C*) or 1 mM $GdCl_3$ (*F*) and harvested at the indicated time points after treatment at ZT0. GI-HA was detected with α-HA antibody. CBB, Coomassie brilliant blue staining.

Salt levels in plants can change within a day, accumulating to high levels during the day, and lower levels at night due to transpiration, and are variable across days with higher levels during sunny days compared to overcast (42–45). Thus, circadian clocks maintain robust and accurate timing over fluctuating environmental factors, including salinity. The transcript and protein abundance of SOS1 exhibits diurnal cycling, with high values during the day (46), which synchronize with salinity levels, supporting a role for SOS1 in salinity compensation. Salt compensation functions in the circadian clock were reported previously for HsfB2b: The circadian period is shortened in the *hsfB2b* mutant under high-salt conditions (e.g., 100 mM NaCl) but not under normal conditions (37). In addition, the salt-dependent short period of *hsfB2b* is enhanced by heat (37). Thus, HsfB2b is likely involved in stress-mediated clock compensation in general. Alternatively, HsfB2b might function as a salt-triggered input signaling to the circadian clock, since its expression has a gated response to salt exposure. Here, we observed that circadian rhythms are dampened in the *sos1* mutant under salt stress (e.g., 100 mM). However, it is not clear whether the loss of circadian rhythmicity in *sos1* is due to the arrest of the circadian clock or loss of vigor. Nevertheless, these results establish SOS1 as a molecular component that buffers the clock against changes in salt levels within the physiological range.

Na^+ ions are among the most abundant soluble minerals, and plants absorb them during water uptake. Exposure to high salinity induces multiple adverse effects, such as osmotic stress and ionic toxicity (17, 28, 30). However, none of these effects recapitulates the salt-induced lengthening of the circadian period and GI degradation in *sos1-1* mutants, except for EGTA (*SI Appendix*, Figs. S6 and S7), indicating the involvement of salt-specific signaling pathways. Salt responses are mediated by crucial secondary signaling messengers, $[Ca^{2+}]_{cyt}$ and ROS (47, 48). $[Ca^{2+}]_{cyt}$ oscillates diurnally, and cADPR forms a transcriptional feedback loop by driving circadian oscillations of Ca^{2+} release (32, 49). The application of calcium to *sos1-1* plants induced GI protein degradation, similarly to NaCl treatment (*SI Appendix*, Fig. S7). Furthermore, applications of two Ca^{2+} antagonists such as nicotinamide and $GdCl_3$ for inhibiting cADPR and Ca^{2+} efflux, respectively, rescued the effect of *sos1* mutation (Fig. 4). Salt stress triggers the rapid production of ROS. A ROS sensor/receptor senses the elevated ROS level and regulates salt responses by activating the downstream pathway and scavenging ROS (30). In addition, waves of ROS and Ca^{2+} are reciprocally integrated to transmit signals, especially abiotic stress signals (50). We also observed that treatment of DMTU, a ROS scavenger, rescued GI stability and lengthened the period in *sos1* plants under salt, similarly to Ca^{2+} inhibitors (*SI Appendix*, Fig. S8). These observations demonstrate that salt-mediated secondary messengers, including $[Ca^{2+}]_{cyt}$ and ROS, are required for the proper function of SOS1 to compensate the circadian clock under salt conditions.

In conclusion, we propose that SOS1 functions in salt-induced responses in plants. Under mild or fluctuating salt conditions, SOS1 stabilizes the phase and period of the circadian clock by directly protecting GI. Under strong or continuous salt stress, plant cells accumulate Na^+ and induce the release of the secondary messenger Ca^{2+} into the cytosol, leading to GI degradation. The release of SOS2 from the GI–SOS2 interaction and

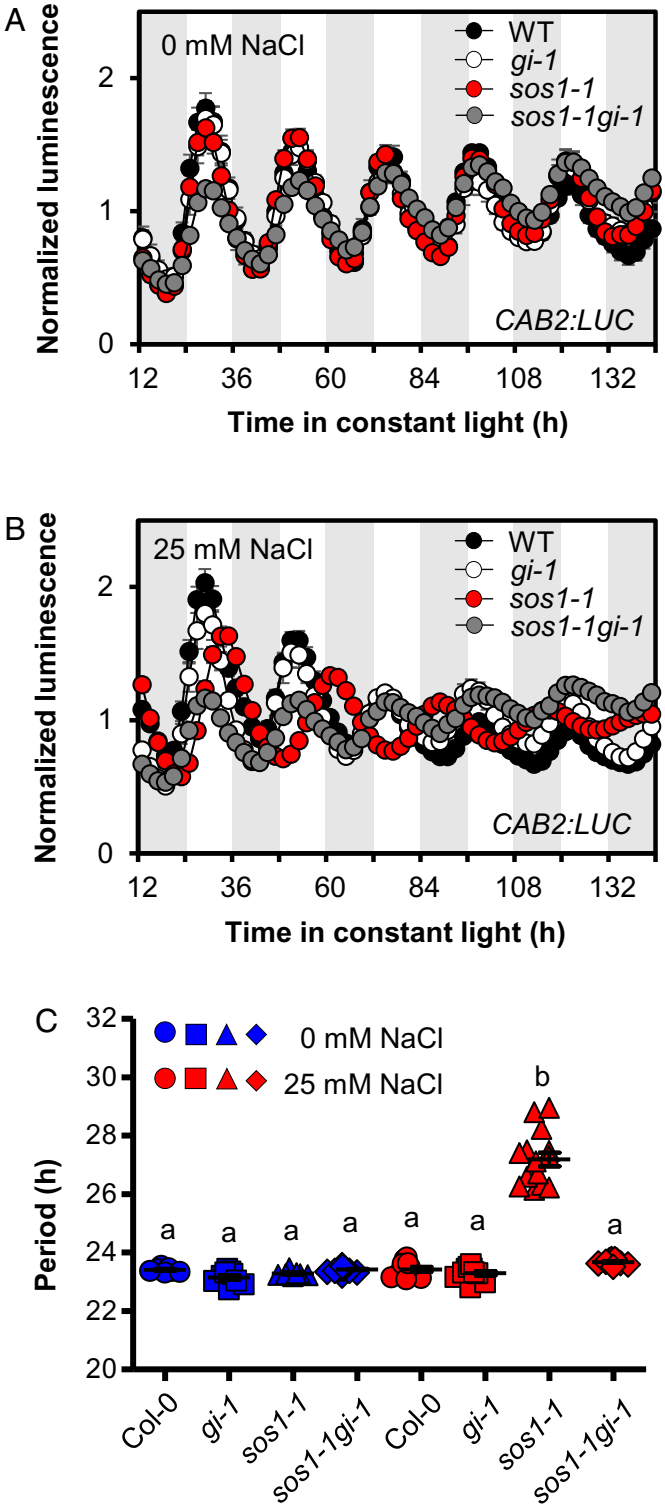

Fig. 5. GI is essential for SOS1-mediated stabilization of circadian period under saline conditions. (*A–C*) Bioluminescence traces (*A* and *B*; means ± SEM) and period estimates (*C*; means ± SEM) of the rhythms of *CAB2-LUC* reporter activity. Different characters indicate significantly different between genotypes or treatments ($P < 0.05$, one-way ANOVA with Tukey's multiple comparisons test). *CAB2:LUC* monitored in WT, *gi-1*, *sos1-1*, and *sos1-1gi-1* seedlings treated with 0 mM NaCl (*A*; $n = 7$, 9, 7, and 14, respectively) or 25 mM NaCl (*B*; $n = 10$, 10, 15, and 9, respectively) under constant blue light (31 μmol m^{-2} s^{-1}). *n* refers to the number of monitored plants.

calcium-dependent activation of SOS3 promote SOS2–SOS3 complex formation and activate the antiporter SOS1 to enhance salt-stress tolerance (Fig. 6). Since salt is one of the most abundant minerals in the soil environment, it would be intriguing to investigate whether the circadian clocks in other organisms beyond plants possess clock compensation mechanisms against salt stress.

Materials and Methods

Plant Materials and Growth Conditions. All mutants and transgenic *Arabidopsis* lines used in this study are in the Columbia (Col) ecotype background (13, 51). Double mutant/transgenic lines including *sos1-1 gi-1*, GI-HA-OX (35S:GI-HA) *sos1-1*, GI-HA-OX *sos2-2*, and GI-HA-OX *sos3-1* were generated by genetic crossing. Mutant/transgenic lines harboring the reporter gene were also created by crossing with reporter lines (*CCA1:LUC* or *CAB2:LUC*). The genotypes were verified by testing antibiotic resistance, PCR, analysis of clock rhythms, or analysis of salt sensitivity. Seeds were germinated and grown on basal medium [1/2 Murashige and Skoog (MS) salts and 3% (wt/vol) sucrose] under a 12-h white light (100 μmol/m^2/s)/12-h dark cycle. For immunoblot analysis and qRT-PCR, 10-d-old seedlings were soaked in NaCl solution at Zeitgeber Time 0 (ZT0) and harvested at the indicated times.

Plasmid Construction. For the immunoprecipitation assays, sequences encoding the middle ($SOS1^{453-670}$, 453 to 670 aa) and C-terminal regions ($SOS1^{671-1146}$, 671 to 1,146 aa) of SOS1 were amplified with Pfu DNA polymerase using specific primer sets ($SOS1^{453-670}$: forward primer 5′-ATGGATATTTTACCAGCCCCC-3′, reverse primer 5′-TCACTGAGGAAATGAAGATCGG-3′; $SOS1^{671-1146}$: forward primer 5′-CTCCGTGTTGTGAAAACAAAAC-3′, reverse primer 5′-TCATAGATCGTTCCTGAAAACG-3′). The resulting PCR products were individually cloned into *pCR8/GW/TOPO* (Invitrogen) to generate entry clones, and the final constructs were generated by LR recombination reaction (Invitrogen) using *pEarleyGate201* or *pMDC43* for GFP fusion. For BiFC analysis, full-length *SOS1* was amplified using a specific primer set (forward primer, 5′- ATGACGACTGTAATCGACGC-3′; reverse primer, 5′-TCATAGATCGTTCCTGAAAACG-3′). For the GST pull-down assay, full-length *GI* was cloned into the *pHis-SUMO* vector, and the sequence encoding the cytoplasmic tail of SOS1 (residues 453 to 1,146) was inserted into *pCR8/GW/TOPO* for entry clones and subcloned into a Gateway version of the *pGEX4T-3* vector by LR recombination reaction.

Bioluminescence Assays in Protoplasts and Transgenic Plants. Bioluminescence was measured in transiently transfected protoplasts as described previously (21). The *CCA1:LUC* reporter plasmids were introduced into *Arabidopsis* protoplasts via polyethylene glycol–mediated transfection, and protoplasts were prepared in W5 solution containing 154 mM NaCl as described previously (21). Bioluminescence in protoplasts was monitored under controlled conditions (Percival E30LEDL3, Percival Scientific) in constant red light (14 μmol m^{-2} s^{-1}) at 23 °C. Images were collected using a Princeton Instruments VersArrayXP:512B digital CCD camera. For bioluminescence analysis in transgenic plants, *Arabidopsis* seedlings harboring reporter genes were grown on 1/2 MS agar medium supplemented with 3% (wt/vol) sucrose for 7 d under a 12-h white light (100 μmol/m^2/s)/12-h dark cycle and transferred to the same medium with or without 25 mM NaCl. After the seedlings were sprayed with D-luciferin (10 μM, Biosynth), bioluminescence images were captured every 2 h for the indicated number of days under constant blue light (31 μmol m^{-2} s^{-1}) at 23 °C using a NightSHADE LB 985 plant imaging system (Berthold Technologies) and IndiGo (ver. 2.0.5.0, Berthold Technologies) software. The amplitude, period, and relative amplitude error of the collected images were estimated with the Fast Fourier Transform-Non-Linear Least Squares method using the Biological Rhythms Analysis software system (BRASS ver. 2.14) as described previously (21, 52). Bioluminescence traces were normalized to the mean expression level over a 12- to 144-h sampling schedule unless indicated.

Immunoblot Analysis and Coimmunoprecipitation (Co-IP). Total proteins were isolated from the samples using protein extraction buffer containing protease and proteasome inhibitors and separated by sodium dodecyl sulfate polyacrylamide gel electrophoresis (SDS-PAGE) as described previously (13). Immunoblot analysis was carried out using rat α-HA antibody (1:2,000; Roche) to detect GI-HA, rabbit α-ZTL antibody (1:500) to detect ZTL (3), and rabbit α-GFP (1:3,000; Abcam) to detect the *TOC1* minigene (53) and SOS1-GFP. To detect native GI protein in *sos1* alleles, soluble proteins were extracted from the

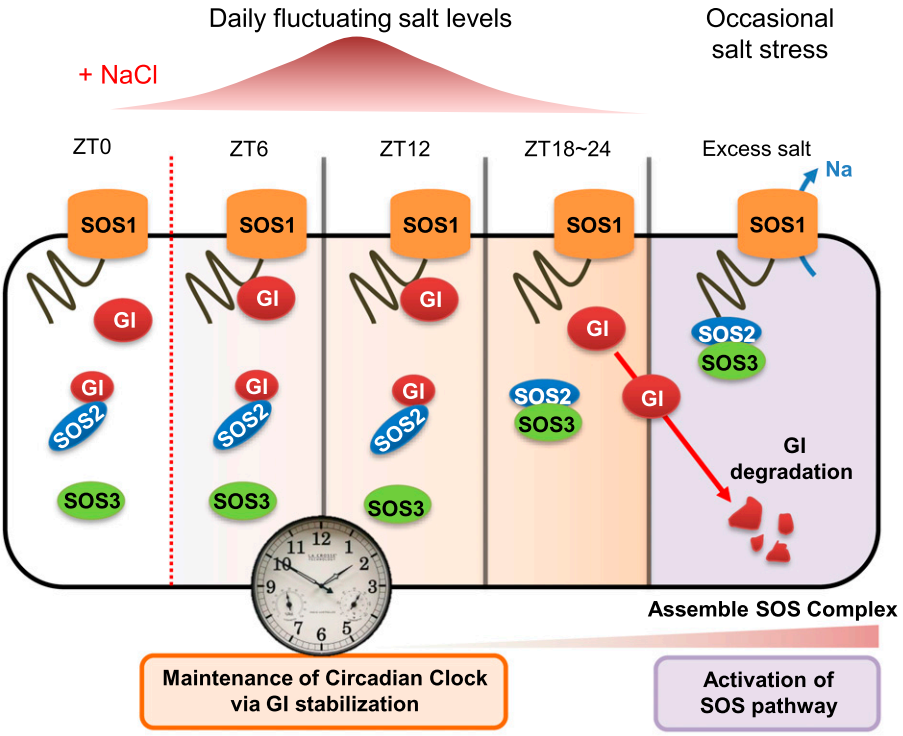

Fig. 6. SOS1 is required for proper circadian clock function in response to changing salinity by controlling GI protein stability. Proposed model of the dual roles of SOS1 in salt compensation and salt tolerance by maintaining proteostasis of GI. Under daily fluctuating salt levels, SOS1 stabilizes GI to maintain circadian clock function. When exposed to high levels of salt, assembly of the SOS complex is initiated by the degradation of GI to enhance salt tolerance; GI degradation induces the recruitment of the SOS2–SOS3 complex to the plasma membrane, which activates the transport activity of the SOS1 antiporter to pump sodium ions out of the cells.

samples using urea/SDS buffer, and immunoblot analysis was performed with rabbit α-GI antibody (54). Proteins were detected based on chemiluminescence using ECL-detecting reagent (Thermo Fisher Scientific) and Chemi-Doc (Bio-Rad). For Co-IP assays, total protein extracts isolated from *N. benthamiana* coexpressing SOS1-GFP and GI-HA were prepared and incubated with Protein A-agarose beads (Invitrogen) to capture α-GFP (for SOS1-GFP, Thermo Fisher Scientific). The immunoprecipitated proteins were separated by SDS-PAGE and detected as described above.

BiFC Assays. *GI* and *SOS1* were fused in-frame to the N-terminal [*pDEST-VYNE(R)GW*, Vn] or C-terminal [*pDEST-VYCE(R)GW*, Vc] fragment of Venus (enhanced yellow fluorescent protein [eYFP] fluorescent protein) using the Gateway system. The constructs were transformed into *Agrobacterium tumefaciens* (GV3101) cells, which were coinfiltrated into the leaves of 3-wk-old *N. benthamiana* plants. After 3-d incubation, 100 mM NaCl or water (0 mM NaCl as a control) was infiltrated into the same leaves at ZT0, and fluorescent signals were detected 6 h later by confocal laser-scanning microscopy (Olympus FV1000, Olympus) with an excitation wavelength of 515 nm for YFP.

GST Pull-Down Assay. To express recombinant His-GI, GST-SOS1$^{453–1146}$, and GST proteins, *Escherichia coli* BL21 (DE3) star cells were transformed with *pHis-SUMO-GI*, *pGEX4T-SOS1*$^{453–1146}$, and *pGEX-2T*, respectively. The transformed cells were grown at 37 °C (optical density$_{600}$ = 0.8). Protein expression was induced by treating the cells with 0.5 mM isopropyl-1-thio-β-$_D$-galactopyranoside (IPTG) for 4 h at 30 °C for GST-SOS1$^{453–1146}$ and GST or 0.1 mM IPTG for 24 h at 15 °C for His-GI. Recombinant proteins were extracted as described previously (5). Supernatants containing GST-SOS1$^{453–1146}$ or GST were immobilized onto Glutathione Sepharose 4 Fast Flow beads (Cytiva) for 2 h at 4 °C, and the beads were washed with cold 1x phosphate-buffered saline (PBS). His-GI protein was purified in Ni-NTA Agarose (Qiagen) using 250 mM imidazole in 1x PBS. GST-SOS1$^{453–1146}$– or GST-bound beads were further incubated with purified His-GI in cold GST lysis buffer (55) for 2 h at 4 °C with rotation. The beads were washed five times with cold GST lysis buffer, resuspended in SDS-PAGE sample buffer, briefly heated at 95 °C for 3 min, and subjected to SDS-PAGE. His-GI bound to GST-SOS1$^{453 – 1146}$ or GST was validated by immunoblot analysis using anti-His antibody (1:500, Thermo Fisher Scientific).

qRT-PCR. Ten-day-old WT (Col-gl) or *sos1-1* seedlings grown under 12-h white light/12-h dark cycle were treated with or without 25 mM NaCl. Total RNA was extracted using an RNeasy kit (Qiagen) according to the manufacturer's instructions. First-strand complementary DNA (cDNA) was synthesized from 2 μg of total RNA using a RevertAid First Strand cDNA Synthesis Kit (Thermo Fisher Scientific) and used for qRT-PCR with a TOPreal qPCR PreMIX Kit (Enzynomics) and a CFX96 Touch Real-Time PCR Detection System (Bio-Rad). The following PCR primer sets were used: *CCA1* forward (5′-CACGGGAAGAGGGAAGTCAG-3′) and *CCA1* reverse (5′- AGGAGGATGTGATAGAGAACTTG-3′); *TOC1* forward (5′-GTACCA ACCTGTTCTCTGACG-3′) and *TOC1* reverse (5′-CAGTAGCAACAGACCACTCAT-3′). Gene expression values for each primer set were normalized to *TUBULIN1* (*TUB1* forward 5′-TGGCATCAACTTTCATTGGA-3′ and reverse 5′-ATGTTGCTCTCCGCTTCTGT-3′) as an internal control. Relative gene expression levels were calculated using the comparative cycle threshold method. All qPCR analyses were performed with three independent biological replicates.

Statistical Analysis. For bioluminescence assays, relative GI level, and qRT-PCR analysis, statistical analysis was assessed as described in the figure legends. Independent experiments were performed at least three times, unless indicated otherwise. Statistical analysis was performed using GraphPad Prism 5.03 version (GraphPad Software) by one-way ANOVA followed by a Tukey's multiple comparisons test ($P < 0.05$). Data are presented as means ± SEM, and P values and sample numbers were as described in the figure legends.

Data Availability. All study data are included in the article and/or *SI Appendix*.

ACKNOWLEDGMENTS. We thank Mi Ri Kim and Andrew Boyles Melencion for their helpful assistance. This work was supported by National Research Foundation of Korea grants funded by the Korean Government (Grant Nos. MSIT 2019R1A2C1088531, 2020R1A2C3014814, and 2022R1A5A1031361 to W.-Y.K. and Grant No. MOE 2019R1A6A1A11052070 to J.K.) and by NIH Grant No. R01GM093285 (to D.E.S.).

Author affiliations: [a]Division of Applied Life Science (BK21four), Plant Molecular Biology and Biotechnology Research Center, Graduate School of Gyeongsang National University, Jinju 52828, Republic of Korea; [b]Research Institute of Life Science, Institute of Agriculture and Life Sciences, Gyeongsang National University, Jinju 52828, Republic of Korea; [c]Faculty of Science Education and Interdisciplinary Graduate Program in Advanced Convergence Technology and Science, Jeju National University, Jeju 63243, Republic of Korea; [d]Department of Molecular Genetics, The Ohio State University, Columbus, OH 43210; [e]Department of Biological Sciences, College of Natural Sciences, Chonnam National University, Gwangju 61186, Republic of Korea; [f]College of Pharmacy, Yeungnam University, Gyeongsan 38541, Republic of Korea; [g]Institute of Plant Biochemistry and Photosynthesis, Consejo Superior de Investigaciones Cientificas and Universidad de Sevilla, Seville 41092, Spain; [h]Department of Biomedical Science and Engineering, Konkuk University, Seoul 05029, Republic of Korea; and [i]Key Laboratory of Molecular Epigenetics of the Ministry of Education, Northeast Normal University, Changchun 130024, China

Author contributions: J.-Y.C., J.K., H.-J.P., S.Y.L., and W.-Y.K. designed research; J.-Y.C., J.K., S.Y.J., G.-I.S., M.G.J., J.-W.H., L.K., X.L., G.A., H.-J.P., and D.Y.K. performed research; J.-Y.C., J.K., G.A., H.-J.P., J.M.P., S.Y.L., D.-J.Y., D.E.S., and W.-Y.K. analyzed data; and J.-Y.C., J.K., J.M.P., D.-J.Y., D.E.S., and W.-Y.K. wrote the paper.

1. C. R. McClung, Plant circadian rhythms. *Plant Cell* **18**, 792–803 (2006).
2. S. E. Sanchez, S. A. Kay, The plant circadian clock: From a simple timekeeper to a complex developmental manager. *Cold Spring Harb. Perspect. Biol.* **8**, a027748 (2016).
3. W.-Y. Kim *et al.*, ZEITLUPE is a circadian photoreceptor stabilized by GIGANTEA in blue light. *Nature* **449**, 356–360 (2007).
4. S. Fujiwara *et al.*, Post-translational regulation of the *Arabidopsis* circadian clock through selective proteolysis and phosphorylation of pseudo-response regulator proteins. *J. Biol. Chem.* **283**, 23073–23083 (2008).
5. J.-Y. Cha *et al.*, GIGANTEA is a co-chaperone which facilitates maturation of ZEITLUPE in the *Arabidopsis* circadian clock. *Nat. Commun.* **8**, 3 (2017).
6. S. F. Boxall *et al.*, Conservation and divergence of circadian clock operation in a stress-inducible Crassulacean acid metabolism species reveals clock compensation against stress. *Plant Physiol.* **137**, 969–982 (2005).
7. N. A. Eckardt, A wheel within a wheel: Temperature compensation of the circadian clock. *Plant Cell* **18**, 1105 (2006).
8. K.-E. Gil, C.-M. Park, Thermal adaptation and plasticity of the plant circadian clock. *New Phytol.* **221**, 1215–1229 (2019).
9. P. D. Gould *et al.*, The molecular basis of temperature compensation in the *Arabidopsis* circadian clock. *Plant Cell* **18**, 1177–1187 (2006).
10. K.-E. Gil *et al.*, ZEITLUPE contributes to a thermoresponsive protein quality control system in *Arabidopsis*. *Plant Cell* **29**, 2882–2894 (2017).
11. T.-S. Kim, L. Wang, Y. J. Kim, D. E. Somers, Compensatory mutations in GI and ZTL may modulate temperature compensation in the circadian clock. *Plant Physiol.* **182**, 1130–1141 (2020).
12. N. Nakamichi *et al.*, Transcript profiling of an *Arabidopsis* PSEUDO RESPONSE REGULATOR arrhythmic triple mutant reveals a role for the circadian clock in cold stress response. *Plant Cell Physiol.* **50**, 447–462 (2009).
13. W.-Y. Kim *et al.*, Release of SOS2 kinase from sequestration with GIGANTEA determines salt tolerance in *Arabidopsis*. *Nat. Commun.* **4**, 1352 (2013).
14. J. Kurepa, J. Smalle, M. Van Montagu, D. Inzé, Oxidative stress tolerance and longevity in *Arabidopsis*: The late-flowering mutant gigantea is tolerant to paraquat. *Plant J.* **14**, 759–764 (1998).
15. T. Legnaioli, J. Cuevas, P. Mas, TOC1 functions as a molecular switch connecting the circadian clock with plant responses to drought. *EMBO J.* **28**, 3745–3757 (2009).
16. A. G. Lai *et al.*, CIRCADIAN CLOCK-ASSOCIATED 1 regulates ROS homeostasis and oxidative stress responses. *Proc. Natl. Acad. Sci. U.S.A.* **109**, 17129–17134 (2012).
17. H. Ji *et al.*, The Salt Overly Sensitive (SOS) pathway: Established and emerging roles. *Mol. Plant* **6**, 275–286 (2013).
18. U. Halfter, M. Ishitani, J. K. Zhu, The *Arabidopsis* SOS2 protein kinase physically interacts with and is activated by the calcium-binding protein SOS3. *Proc. Natl. Acad. Sci. U.S.A.* **97**, 3735–3740 (2000).
19. H. Shi, M. Ishitani, C. Kim, J. K. Zhu, The *Arabidopsis thaliana* salt tolerance gene SOS1 encodes a putative Na^+/H^+ antiporter. *Proc. Natl. Acad. Sci. U.S.A.* **97**, 6896–6901 (2000).
20. L.-H. Cho, J. Yoon, G. An, The control of flowering time by environmental factors. *Plant J.* **90**, 708–719 (2017).
21. J. Kim, D. E. Somers, Rapid assessment of gene function in the circadian clock using artificial microRNA in *Arabidopsis* mesophyll protoplasts. *Plant Physiol.* **154**, 611–621 (2010).
22. R. Schaffer *et al.*, The late elongated hypocotyl mutation of *Arabidopsis* disrupts circadian rhythms and the photoperiodic control of flowering. *Cell* **93**, 1219–1229 (1998).
23. Z.-Y. Wang, E. M. Tobin, Constitutive expression of the *CIRCADIAN CLOCK ASSOCIATED 1* (*CCA1*) gene disrupts circadian rhythms and suppresses its own expression. *Cell* **93**, 1207–1217 (1998).
24. D. H. Park *et al.*, Control of circadian rhythms and photoperiodic flowering by the *Arabidopsis* GIGANTEA gene. *Science* **285**, 1579–1582 (1999).
25. D. E. Somers, T. F. Schultz, M. Milnamow, S. A. Kay, ZEITLUPE encodes a novel clock-associated PAS protein from *Arabidopsis*. *Cell* **101**, 319–329 (2000).
26. R. Núñez-Ramírez *et al.*, Structural insights on the plant Salt-Overly-Sensitive 1 (SOS1) Na^+/H^+ antiporter. *J. Mol. Biol.* **424**, 283–294 (2012).
27. F. J. Quintero *et al.*, Activation of the plasma membrane Na/H antiporter Salt-Overly-Sensitive 1 (SOS1) by phosphorylation of an auto-inhibitory C-terminal domain. *Proc. Natl. Acad. Sci. U.S.A.* **108**, 2611–2616 (2011).
28. S. V. Isayenkov, F. J. M. Maathuis, Plant salinity stress: Many unanswered questions remain. *Front. Plant Sci.* **10**, 80 (2019).
29. J.-K. Zhu, Abiotic stress signaling and responses in plants. *Cell* **167**, 313–324 (2016).
30. Y. Yang, Y. Guo, Unraveling salt stress signaling in plants. *J. Integr. Plant Biol.* **60**, 796–804 (2018).
31. K. H. Edel, E. Marchadier, C. Brownlee, J. Kudla, A. M. Hetherington, The evolution of calcium-based signalling in plants. *Curr. Biol.* **27**, R667–R679 (2017).
32. A. N. Dodd *et al.*, The *Arabidopsis* circadian clock incorporates a cADPR-based feedback loop. *Science* **318**, 1789–1792 (2007).
33. J. K. Sethi, R. M. Empson, A. Galione, Nicotinamide inhibits cyclic ADP-ribose-mediated calcium signalling in sea urchin eggs. *Biochem. J.* **319**, 613–617 (1996).
34. A.-A. Véry, J. M. Davies, Hyperpolarization-activated calcium channels at the tip of *Arabidopsis* root hairs. *Proc. Natl. Acad. Sci. U.S.A.* **97**, 9801–9806 (2000).
35. P. Mishra, K. C. Panigrahi, GIGANTEA – An emerging story. *Front. Plant Sci.* **6**, 8 (2015).
36. R. Munns, M. Tester, Mechanisms of salinity tolerance. *Annu. Rev. Plant Biol.* **59**, 651–681 (2008).
37. E. Kolmos, B. Y. Chow, J. L. Pruneda-Paz, S. A. Kay, HsfB2b-mediated repression of PRR7 directs abiotic stress responses of the circadian clock. *Proc. Natl. Acad. Sci. U.S.A.* **111**, 16172–16177 (2014).
38. H. El Mahi *et al.*, A critical role of sodium flux via the plasma membrane Na^+/H^+ exchanger SOS1 in the salt tolerance of rice. *Plant Physiol.* **180**, 1046–1065 (2019).
39. B. Moore *et al.*, Role of the *Arabidopsis* glucose sensor HXK1 in nutrient, light, and hormonal signaling. *Science* **300**, 332–336 (2003).
40. C.-H. Ho, S.-H. Lin, H.-C. Hu, Y.-F. Tsay, CHL1 functions as a nitrate sensor in plants. *Cell* **138**, 1184–1194 (2009).
41. E. Bouguyon *et al.*, Nitrate controls root development through posttranscriptional regulation of the NRT1.1/NPF6.3 transporter/sensor. *Plant Physiol.* **172**, 1237–1248 (2016).
42. M. A. Caird, J. H. Richards, L. A. Donovan, Nighttime stomatal conductance and transpiration in C3 and C4 plants. *Plant Physiol.* **143**, 4–10 (2007).
43. F. Lopez *et al.*, Diurnal regulation of water transport and aquaporin gene expression in maize roots: Contribution of PIP2 proteins. *Plant Cell Physiol.* **44**, 1384–1395 (2003).
44. S. Siebrecht, K. Herdel, U. Schurr, R. Tischner, Nutrient translocation in the xylem of poplar–Diurnal variations and spatial distribution along the shoot axis. *Planta* **217**, 783–793 (2003).
45. G. P. Ruwanpathirana *et al.*, Continuous monitoring of plant sodium transport dynamics using clinical PET. *Plant Methods* **17**, 8 (2021).
46. H. J. Park, Z. Qiang, W.-Y. Kim, D.-J. Yun, Diurnal and circadian regulation of salt tolerance in *Arabidopsis*. *J. Plant Biol.* **59**, 569–578 (2016).
47. G. Miller *et al.*, The plant NADPH oxidase RBOHD mediates rapid systemic signaling in response to diverse stimuli. *Sci. Signal.* **2**, ra45 (2009).
48. W.-G. Choi, M. Toyota, S.-H. Kim, R. Hilleary, S. Gilroy, Salt stress-induced Ca^{2+} waves are associated with rapid, long-distance root-to-shoot signaling in plants. *Proc. Natl. Acad. Sci. U.S.A.* **111**, 6497–6502 (2014).
49. J. Love, A. N. Dodd, A. A. R. Webb, Circadian and diurnal calcium oscillations encode photoperiodic information in *Arabidopsis*. *Plant Cell* **16**, 956–966 (2004).
50. S. Gilroy *et al.*, ROS, calcium, and electric signals: Key mediators of rapid systemic signaling in plants. *Plant Physiol.* **171**, 1606–1615 (2016).
51. J. Liu, J.-K. Zhu, An *Arabidopsis* mutant that requires increased calcium for potassium nutrition and salt tolerance. *Proc. Natl. Acad. Sci. U.S.A.* **94**, 14960–14964 (1997).
52. D. E. Somers, W.-Y. Kim, R. Geng, The F-box protein ZEITLUPE confers dosage-dependent control on the circadian clock, photomorphogenesis, and flowering time. *Plant Cell* **16**, 769–782 (2004).
53. P. Más, D. Alabadí, M. J. Yanovsky, T. Oyama, S. A. Kay, Dual role of TOC1 in the control of circadian and photomorphogenic responses in *Arabidopsis*. *Plant Cell* **15**, 223–236 (2003).
54. L. Khaleda, J.-Y. Cha, M. G. Kim, W.-Y. Kim, Production and characterization of polyclonal antibody against Arabidopsis GIGANTEA, a circadian clock controlled flowering time regulator. *J. Plant Biol.* **60**, 622–629 (2017).
55. Detection of protein-protein interactions using the GST fusion protein pull-down technique. *Nat. Methods* **1**, 275–276 (2004).